

High-Resolution Length Sorting and Purification of DNA-Wrapped Carbon Nanotubes by Size-Exclusion Chromatography

Xueying Huang,[†] Robert S. Mclean,[‡] and Ming Zheng^{*†‡}

Sepax Technologies, Inc., Newark, Delaware 19711, and DuPont Central Research and Development, Wilmington, Delaware 19880

We report a size-exclusion chromatography (SEC) process to purify DNA-wrapped carbon nanotubes (DNA-CNT) and to sort them into fractions of uniform length. A type of silica-based column resin was identified that shows minimum adsorption of DNA-CNT. Three such columns in series with pore sizes of 2000, 1000, and 300 Å were found to separate DNA-CNT into fractions of very narrow length distribution, as measured directly by atomic force microscopy. The average length decreases monotonically from >500 nm in the early fractions to <100 nm in the late fractions, with length variation $\leq 10\%$ in each of the measured fractions. Using UV–vis–NIR spectroscopy, we showed that SEC is very effective in removing graphitic impurities that contribute to the spectral baseline and a broad absorption peak at ~ 270 nm. This result highlights the importance of CNT purification in the study of optical properties of CNT.

The dominant physical dimension of a single-walled carbon nanotube (CNT) is its length. As a one-dimensional material, the electronic band structure of a CNT is not dependent on its length.¹ However, certain physical processes, such as carrier recombination, could still be length-dependent. Device applications, such as CNT-based scanning probes, require CNT length control for easy and reproducible fabrication. Solution-phase CNT processing, ranging from separation of CNTs by their diameters and chiralities to assembly of CNTs on solid substrates, are also expected to benefit from CNTs of well-defined length.

Many studies have been done on length sorting. Methods reported include capillary electrophoresis,^{2,3} gel electrophoresis,⁴ and size-exclusion chromatography.^{4–8} In many of the reported

works, quantification of length variation in obtained fractions was absent. Some works did demonstrate control over the average length of separated tubes; the length variation within a given fraction, however, was typically very broad and could be as high as 80%. In addition, some of the processes reported cannot be scaled up for processing large quantities of materials. It is, thus, highly desirable to develop a scalable process that can yield CNT fractions of well-defined length.

We have shown previously that single-stranded DNA (ssDNA) wraps around CNT to form a DNA-CNT hybrid and effectively disperses CNT into aqueous solution.⁹ Sorting CNTs by their diameters and chirality has also been demonstrated using DNA-CNT dispersions.^{10,11} The structurally sorted DNA-CNT materials have served as valuable tools for elucidating the fundamental physical and chemical properties of CNT.^{11–13} In this work, we further demonstrate that DNA-CNTs can be separated using conventional size-exclusion chromatography to yield populations of nanotubes with well-defined length. Using UV–vis–NIR spectroscopy, we show that SEC is also very effective in removing graphitic impurities that contribute to the spectral baseline and a broad absorption peak at ~ 270 nm. These results further illustrate the utility of DNA-CNTs in CNT material processing and highlight the importance of CNT purification in the study of physical properties of CNTs.

* Corresponding author. Fax: 302-695-8909. E-mail: ming.zheng@usa.dupont.com.

[†] Sepax Technologies, Inc.

[‡] DuPont Central Research and Development.

- (1) Saito, R.; Dresselhaus, G.; Dresselhaus, M. S. *Physical Properties of Carbon Nanotubes*; Imperial College Press: London, 1999.
- (2) Doorn, S. K.; Fields, R. E., III; Hu, H.; Hamon, M. A.; Haddon, R. C.; Selegue, J. P.; Majidi, V. *J. Am. Chem. Soc.* **2002**, *124*, 3169–3174.
- (3) Doorn, S. K.; Strano, M. S.; O'Connell, M. J.; Haroz, E. H.; Rialon, K. L.; Hauge, R. H.; Smalley, R. E. *J. Phys. Chem. B* **2003**, *107*, 6063–6069.
- (4) Heller, D. A.; Mayrhofer, R. M.; Baik, S.; Grinkova, Y. V.; Usrey, M. L.; Strano, M. S. *J. Am. Chem. Soc.* **2004**, *126*, 14567–14573.
- (5) Duesberg, G. S.; Blau, W.; Byrne, H. J.; Muster, J.; Burghard, M.; Roth, S. *Synth. Met.* **1999**, *103*, 2484–2485.

- (6) Chattopadhyay, D.; Lastella, S.; Kim, S.; Papadimitrakopoulos, F. *J. Am. Chem. Soc.* **2002**, *124*, 728–729.
- (7) Niyogi, S.; Hu, H.; Hamon, M. A.; Bhowmik, P.; Zhao, B.; Rozenzhak, S. M.; Chen, J.; Itkis, M. E.; Meier, M. S.; Haddon, R. C. *J. Am. Chem. Soc.* **2001**, *123*, 733–734.
- (8) Farkas, E.; Anderson, M. E.; Chen, Z.; Rinzler, A. G. *Chem. Phys. Lett.* **2002**, *363*, 111–116.
- (9) Zheng, M.; Jagota, A.; Semke, E. D.; Diner, B. A.; McLean, R. S.; Lustig, S. R.; Richardson, R. E.; Tassi, N. G. *Nat. Mater.* **2003**, *2* (5), 338–342.
- (10) Zheng, M.; Jagota, A.; Strano, M. S.; Santos, A. P.; Barone, P.; Chou, S. G.; Diner, B. A.; Dresselhaus, M. S.; McLean, R. S.; Onoa, G. B.; Samsonidze, G. G.; Semke, E. D.; Usrey, M.; Walls, D. J. *Science* **2003**, *302* (5650), 1545–1548.
- (11) Zheng, M.; Diner, B. A. *J. Am. Chem. Soc.* **2004**, *126* (47), 15490–15494.
- (12) Chou, S. G.; Ribeiro, H. B.; Barros, E. B.; Santos, A. P.; Nezhich, D.; Samsonidze, G. G.; Fantinib, C.; Pimenta, M. A.; Jorio, A.; Plentz Filho, F.; Dresselhaus, M. S.; Dresselhaus, G.; Saito, R.; Zheng, M.; Onoa, G. B.; Semke, E. D.; Swan, A. K.; Ünlü, M. S.; Goldberg, B. B. *Chem. Phys. Lett.* **2004**, *397* (4–6), 296–301.
- (13) Chou, S. G.; Plentz, F.; Jiang, J.; Saito, R.; Nezhich, D.; Ribeiro, H. B.; Jorio, A.; Pimenta, M. A.; Samsonidze, G. G.; Santos, A. P.; Zheng, M.; Onoa, G. B.; Semke, E. D.; Dresselhaus, G.; Dresselhaus, M. S. *Phys. Rev. Lett.* **2005**, *94*, 127402.

EXPERIMENTAL SECTION

Single-walled carbon nanotubes used in this study are the CoMoCAT nanotubes purchased from Southwest Nanotechnologies (Norman, OK). The CoMoCAT tubes have relatively narrow diameter distribution and are well-suited for our separation studies. Single-stranded DNA sequence, d(GT)₃₀, custom-made by Integrated DNA Technologies, Inc. (Coralville, IA), was used for CNT dispersion. All other chemicals were purchased from Sigma-Aldrich (St. Louis, MO) unless otherwise specified. CNT dispersion by ssDNA was conducted according to procedures described previously.⁹

Size-exclusion columns were purchased from Sepax Technologies, Inc. (Newark, DE). The stationary phase is 5- μ m silica beads with pore sizes ranging from 300 to 2000 Å. The surface functional groups on the beads bear negative charges to prevent nonspecific adsorption by the negatively charged DNA-CNTs. For experiments reported in this paper, three columns in the order of CNT SEC-2000, CNT SEC-1000, and CNT SEC-300 with pore sizes of 2000, 1000, and 300 Å, respectively, were connected in series and mounted on a BioCAD/Sprint HPLC system (Applied Biosystems). The HPLC system uses a flow cell (3-mm path length and 4.6- μ L volume) to measure optical absorption from the elution at a single wavelength in the range of 190–380 nm. The column dimensions were chosen according to the amount of materials to be processed. For analytical work, column dimensions were 4.6 mm \times 250 mm. For large-scale separation with 5-mL loading, 21 mm \times 250 mm columns were used. In a typical analytical run, 200 μ L of stock DNA-CNT solution at a concentration of \sim 0.3 mg/mL was loaded onto the column series and eluted with a pH 7 buffer containing 40 mM Tris, 0.5 mM EDTA, and 0.2 M NaCl at a flow rate of 0.25 mL/min. Elution was collected at 0.25 mL/fraction.

We chose chlorodimethylethylsilane (C2)-coated SiO₂ on Si as the substrate for AFM sample deposition, which was prepared as follows: Silicon chips were first cleaned with piranha solution (70 vol % H₂SO₄ + 30 vol % H₂O₂). Cleaned silicon chips were then placed in a Pyrex kettle and mixed with 200 mL of toluene, 10 mL of chlorodimethylethylsilane (97% from Aldrich), and 3 mL of pyridine. The mixture was refluxed in an oil bath for 5 h with stirring. The reacted chips were then rinsed with toluene, acetone, and methanol, twice for each, and baked in an oven at 110 °C for 1 h. Measured advancing and receding water contact angles of the coated surface are \sim 100 and \sim 90°, respectively.

Samples used for AFM measurement were prepared as follows: SEC fractions were exchanged into a pH 7 buffer made of 10 mM Tris/0.5 mM EDTA to yield a final nanotube concentration of \sim 1 μ g/mL. Buffer exchange was performed using a Microcon centrifugal filter YM-100 (Millipore, Bedford, MA). In a typical experiment, a 10- μ L drop of the prepared DNA-CNT solution was deposited on a C2-coated SiO₂ surface. After 15 min of incubation at ambient conditions, the drop was rinsed away with deionized water, and the substrate was dried with nitrogen gas.

AFM was then used to visualize DNA-CNTs adsorbed onto the substrate. Measurements were conducted in air using the tapping mode on a Nanoscope IIIa AFM, Dimension 3000 from Digital Instruments (Santa Barbara, CA). Microfabricated cantilevers or silicon probes (Nanoprobes, Digital Instruments) with

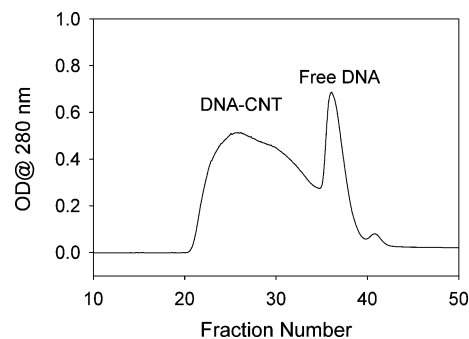


Figure 1. Chromatogram of size-exclusion column separation of DNA-CNT. A 200 μ L portion of stock DNA-CNT solution at a concentration of \sim 0.3 mg/mL was loaded onto a three-column series, as described in the Experimental Section, and eluted with 40 mM Tris pH 7, 0.5 mM EDTA, and 0.2 M NaCl at a flow rate of 0.25 mL/min. Elution was collected at 0.25 mL/fraction. "OD @ 280 nm" denotes optical density measured at 280 nm by the HPLC flow cell.

125- μ m-long cantilevers were used at their fundamental resonance frequencies. These cantilevers have tip radii of 5–10 nm. The images presented here are not filtered.

UV–vis–NIR spectroscopy was conducted using a 10-mm optical path length quartz cell. Before sample measurement, DNA-CNT solutions were exchanged into H₂O using a Microcon centrifugal filter YM-100. This ensures removal of free DNA and other organic components that have absorption in the UV region.

RESULTS AND DISCUSSION

Choice of Size-Exclusion Column. SEC is a widely used technique for fractionating macromolecules according to their physical sizes. For a given column pore size, a larger molecule (relative to the pore size) encounters larger excluded volume when passing through the column and, therefore, has a shorter retention time. However, if the molecule is too large or too small, the size-exclusion effect becomes less sensitive. A common strategy to fractionate objects with broad size distribution is to pass them through several columns with different pore sizes. Since the dominating physical dimension for a CNT is its length, SEC is expected to result in length but not diameter fractionation, consistent with our findings.

There are many types of size-exclusion columns that are commercially available. We have found that most of them are not suited for the separation of DNA-CNT materials. A common problem is the irreversible adsorption of the DNA-CNT on the stationary phase. The specially designed Sepax CNT-SEC columns, on the other hand, have near 100% recovery of the loaded DNA-CNT materials and are well-suited for our separation purpose. Depending on the amount of the materials that need to be separated, we chose different size columns. With a stock concentration of \sim 0.3 mg/mL, we used a 4.6-mm-diameter column for 200- μ L loading, a 10-mm-diameter column for 1-mL loading, and a 21.2-mm-diameter column for 5-mL loading. The CNT length resolution was found to be dependent on the choice of the pore size of the column resin. With a single 2000-Å pore size column, we found that tubes longer than 500 nm were well-resolved. Conversely, if a single 300-Å pore size column was used, tubes shorter than 200 nm were well-resolved. To obtain uniform length distribution for both shorter and longer tube fractions, we have tested a three-column series in which the first, second, and the

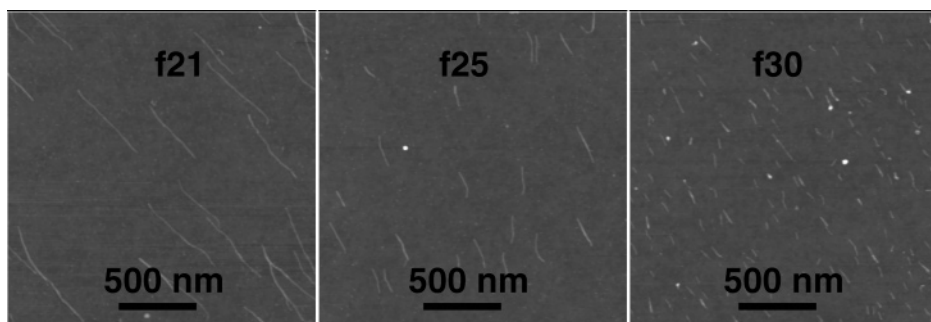


Figure 2. AFM images of three representative SEC fractions deposited onto alkyl silane-coated SiO₂ substrates.

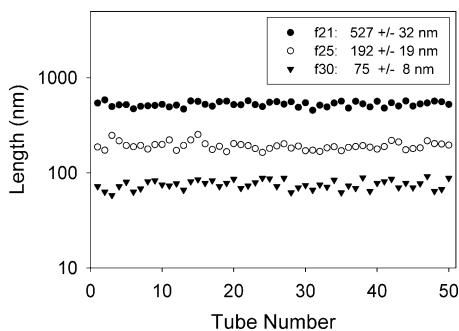


Figure 3. Statistical analysis of tube length distribution in different SEC fractions. Length measurement was performed directly from the AFM images of the SEC fractions. A total of 50 randomly chosen tubes from each fraction were measured, and their lengths were plotted using log scale. The result is given as mean \pm standard deviation.

third columns have pore sizes of 2000, 1000, and 300 Å, respectively. This column configuration, indeed, yielded the best results. All the data shown in this paper were therefore obtained by using the three-column series.

Length Separation by SEC. A typical elution profile from the three-column series is shown in Figure 1. After a void volume, DNA-CNTs of different length are eluted. On the basis of its UV-vis spectrum, the relatively narrower peak at \sim 37 min retention time (corresponding to fraction 37) is identified as free DNA. To quantify length distribution of tubes in each SEC fraction, we deposited DNA-CNTs on an alkyl silane-modified SiO₂ substrate and used AFM to directly measure the tube length. Results from three representative fractions are shown in Figure 2. As can be seen, from early to late fractions, there is a clear decrease in the average tube length. To quantify the average length and length variation in each fraction, we randomly picked 50 tubes from the AFM images of each fraction and measured their lengths. These data are shown in Figure 3. A statistical analysis gives (mean \pm standard deviation) 527 \pm 32 nm, 192 \pm 19 nm, and 75 \pm 8 nm for f21, f25, and f30, respectively. The length variation is typically 10% or less for each of the measured fractions. This is considerably better than 30–80% variation reported in the literature.^{4,8} The measured heights of the DNA-CNTs are typically in the range of 1.2–1.4 nm and do not vary significantly from fraction to fraction.

Impurity Removal by SEC. UV-vis-NIR spectroscopy is a powerful tool to analyze singly dispersed carbon nanotube solutions. It records optical transitions between van Hove singularities from both metallic and semiconducting tubes, and the absorption peaks from the semiconducting tubes can be used to deduce their structures.¹⁴ UV-vis-NIR analysis of our SEC fractions revealed

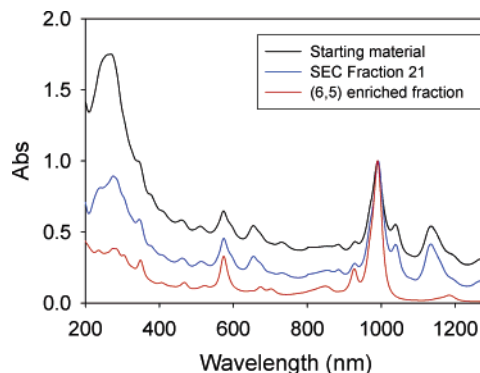


Figure 4. UV-vis-NIR absorption spectra of the starting material, f21 of the SEC separation described in the text, and a (6,5) enriched fraction obtained by ion-exchange chromatography. All samples were exchanged into H₂O for the measurement. Spectral intensities are normalized to 1 at 990 nm.

an interesting phenomenon not reported by previous works. The unfractionated starting material has a featureless baseline that decays monotonically from 300 to 1300 nm and beyond. This feature is common to all the dispersed nanotube solutions regardless of the dispersing agents and the type of tubes. Associated with this rolling down baseline is a strong peak at \sim 270 nm (4.6 eV), which is also observed in the absorption spectra of CNT dispersions and CNT films obtained by others. In all previous works reported by other groups, this peak was by far the most dominant one, \sim 5 to 10 times stronger than the band-gap transitions. In comparison, the intensity of the 270-nm feature in our DNA-CNT starting material is relatively low, \sim 2 times of that of the E₁₁ features at \sim 990 nm (Figure 4, black trace). We found that SEC separation dramatically reduces the 270-nm peak intensity and the baseline level. The intensity of the 270-nm feature in the SEC f21 fraction (Figure 4, blue trace) is reduced by \sim 2-fold in comparison with the starting material. As a result, a few partially resolved peaks around 270 nm can now be observed. In addition, the baseline level in the visible and near-IR region is also reduced by \sim 2-fold. For comparison, we also show in Figure 4 the spectrum of a (6,5) enriched fraction purified from the starting material by ion exchange (IEX) chromatography (red trace) according to procedures described previously.¹¹ As can be seen, the (6,5) enriched fraction has the lowest baseline level among all three samples shown. The 270-nm feature present at high intensities in both the starting material and the SEC f21 is almost absent in the (6,5) enriched fraction. Note that ssDNA

(14) Bachilo, S. M.; Strano, M. S.; Kittrell, C.; Hauge, R. H.; Smalley, R. E.; Weisman, R. B. *Science* **2002**, *298*, 2361–2366.

absorbs in the UV region with an absorption peak at 260 nm, the intensity of which is such that one absorption unit at 260 nm is equivalent to 33 μg DNA/mL. Since the concentration of the wrapping DNA in the (6,5) enriched fraction is estimated to be 5 $\mu\text{g}/\text{mL}$, we conclude that the wrapping DNA is primarily responsible for the small residual absorption peak at ~ 270 nm in the (6,5) enriched fraction. Combining both the SEC and the IEX results, we conclude that the spectral baseline and the 270-nm feature are mostly given by impurities, which can be effectively removed by SEC and IEX chromatography. Since SEC has higher recovery and is easier to scale-up, it can be used as the first step in CNT purification and separation.

Origin of the Impurities. Our assignment of the 270-nm feature to non-single-walled CNT sources contrasts to the prevailing understanding of previous workers. This feature was either attributed to carbon nanotube π plasmon absorption or described as a common optical feature of graphite materials shared by carbon nanotubes.^{15–17} However, none of the previous assignment was deduced from measurements of highly purified CNT samples. On the basis of our SEC and IEX results, we propose that the broad peak around 270 nm and the baseline are largely due to the graphitic impurities coming from original CNT synthesis, from broken nanotube fragments generated by sonication during dispersion process, or from both. Indeed, we observed that the baseline level and the 270-nm peak are increased by longer sonication. Since graphitic fragments are expected to be shorter than long and intact carbon nanotubes, SEC provides an efficient way to remove these impurities. The longer the nanotubes, the larger the difference in retention time between the tubes and the impurities. Consistent with this, we also found that the baseline level and the 270-nm peak gradually increase from early to late SEC fractions, indicating that impurities were eluted primarily in

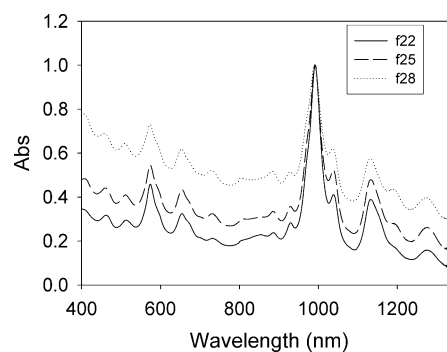


Figure 5. UV–vis–NIR absorption spectra of f22, f25, and f28 from the SEC separation described in the text. All samples were exchanged into H_2O for the measurement. Spectral intensities are normalized to 1 at 990 nm.

the later SEC fractions. Figure 5 illustrates this observation with UV–vis–NIR spectra from three representative fractions. For comparison, all the spectra are normalized at the wavelength where the strongest E_{11} peak occurs. An alternative explanation is that length variation from early to late fractions is responsible for the observed changes in the baseline level and the 270-nm peak intensity. However, this is not consistent with the fact that the (6,5) enriched fraction has the lowest baseline level and 270-nm peak intensity, even though the tube length varies from 100 to 500 nm in the (6,5) enriched fraction. We cannot exclude multiwall or bundled single-walled carbon nanotubes as one of the sources of the 270-nm feature and the baseline.

ACKNOWLEDGMENT

We thank Ms. Ellen D. Semke for technical support. This work comes from the Molecular Electronics Group at DuPont Central Research and Development.

Received for review May 21, 2005. Accepted July 25, 2005.

AC0508954

(15) Kataura, H.; Kumazawa, Y.; Maniwa, Y.; Umezub, I.; Suzukic, S.; Ohtsukac, Y.; Achiba, Y. *Synth. Met.* **1999**, *103*, 2555–2558.

(16) Pichler, T.; Knupfer, M.; Golden, M. S.; Fink, J.; Rinzler, A.; Smalley, R. E. *Phys. Rev. Lett.* **1998**, *80*, 4729–4732.

(17) Murakami, Y.; Einarsson, E.; Edamura, T.; Maruyama, S. *Phys. Rev. Lett.* **2005**, *94*, 087402.